Preprints.org

Article

Exploring Conformational Transitions in Biased and Balanced Ligand Binding of GLP-1R

Marc Xu , Horst Vogel , Shuguang Yuan *

Article

Exploring Conformational Transitions in Biased and Balanced Ligand Binding of GLP-1R

Marc Xu [1,2], Horst Vogel [1,3,4],* and Shuguang Yuan [1,5,*]

[1] Research Center for Computer-Aided Drug Discovery, Shenzhen Institutes of Advanced Technology, Chinese Academy of Sciences, Shenzhen, 518055, Guangdong, China

[2] University of Chinese Academy of Sciences, Beijing 100049, China

[3] Faculty of Pharmaceutical Sciences, Shenzhen University of Advanced Technology, Shenzhen, 518055, Guangdong, China

[4] Institut des Sciences et Ingénierie Chimiques (ISIC), Ecole Polytechnique Fédérale de Lausanne (EPFL), Lausanne, Switzerland

[5] AlphaMol Science Ltd, Shenzhen 518055, Guangdong, China

* Correspondence: horst.vogel@epfl.ch (H.V.); shuguang.yuan@cadd2drug.org (S.Y.)

Abstract: The glucagon-like peptide-1 receptor (GLP-1R), which belongs to the class B1 G protein-coupled receptor (GPCR) family, is an important target for treatment of metabolic disorders including type 2 diabetes and obesity. The growing interest of GLP-1R-based therapies is driven by the development of various functional agonists as well as the huge commercial market. Thus, understanding the structural details of the ligand-induced signaling are important for developing improved GLP-1R drugs. Here, we investigated the conformational dynamics of the receptor in complex with a selection of prototypical functional agonists, including CHU-128 (SM biased), danuglipron (SM balanced), and Peptide 19 (peptide balanced), which exhibit unique, distinct binding modes and induced helix packing. Furthermore, our all-atom molecular dynamics (MD) simulations revealed atomic feature how different those ligands led to signaling pathway preference. Our findings offer valuable insights into the mechanistic principle of GLP-1R activation, which are helpful for the rational design of next-generation GLP-1R drug molecules.

Keywords: GLP-1R signaling; conformational dynamics; structural analyses; molecular dynamics simulation

Introduction

G protein-coupled receptors (GPCRs) are important mediators of extracellular signals across the cell's plasma membrane, conveying external stimuli to intracellular effectors that regulate various cellular processes. The activation process of GPCRs is driven by an internal network of interacting residues which coordinates conformational transitions between the functional states of the receptor. Structural elucidation of receptor-ligand complexes has provided valuable insights into the important interaction networks that trigger specific signaling pathways [1]. Recent advances in determination GPCR structures have significantly enhanced our understanding of the receptor functions and fostered the structure-based drug discovery of GPCR drugs. Yet, the experimentally determined GPCR structures often failed to capture the full inherent flexibility of GPCRs, as they typically represent a very limited number of static snapshots of the receptor's large dynamic conformational landscape in the activation process [2]. To better understand the receptors' functional transitions and conformational dynamics, the static structures of the receptor in specific activation state serve as a constitutive basis for *in silico* simulation of the entire GPCR activation process [2–4].

In recent years, glucagon like peptide 1 (GLP-1) receptor have gained considerable attention as a target for the clinical treatment of metabolic disorders, particularly of type 2 diabetes (T2D) and obesity. GLP-1R belongs the secretin-like family of class B GPCRs, which is predominantly expressed
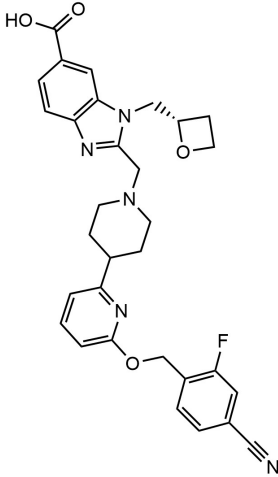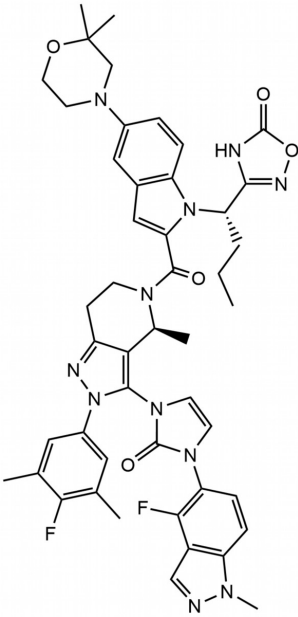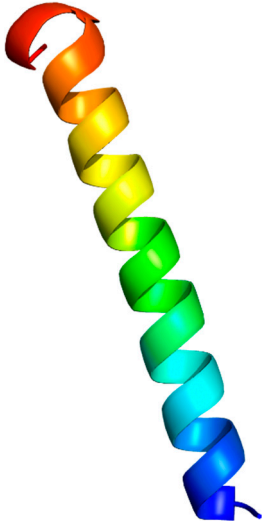
in pancreatic β-cells. It controls both insulin and glucagon secretion in glucose-dependent manner [5]. Activation of GLP-1R induces insulin secretion, inhibits glucagon secretion, and slows gastric emptying, thus contributing to the central regulation of blood glucose levels. Dysfunctional GLP-1R activation disrupts metabolic homeostasis, contributing to the pathogenesis of metabolic diseases[6]. However, the administration of GLP-1R agonists (GLP-1RAs) in T2D patients has been shown to improve glycemic control [7–10].

Over the past few decades, numerous GLP-1RAs, such as semaglutide and liraglutide, have been developed, featuring intrinsic modification of the native GLP-1 peptide to imitate the pharmacological profile of GLP-1, while providing resistance to degradation by the enzyme dipeptidyl peptidase-4 [11–13]. Interestingly, these molecules have demonstrated extended therapeutic benefits, including potential applications in cardiovascular diseases and neurodegenerative diseases, as well as in non-alcoholic fatty liver disease [6,14–16]. Despite their efficacy, some GLP-1RAs exhibit reduced therapeutic effects due to undesired receptor trafficking, attenuating the glucoregulatory responses by desensitization and downregulation caused by β-arrestin recruitment [17,18]. To overcome this limitation, the development of G_s-biased agonists has been pursued, which enhance insulin release in cell-based experiments by selectively amplifying cAMP signaling [19]. Further evidences have been delivered showing that the administration of G_s-biased agonists are more effective than cAMP and β-arrestin 2 signaling balanced agonists in regulation glucose homeostasis and bodyweight control in mice [20,21]. However, additional clinical studies are essential to fully evaluate the long-term implications of selective signaling modulation [22].

Furthermore, peptide GLP-1RAs are typically administrated via injection, which leads to challenge of patient compliance, gastrointestinal side effects, and production costs [23–26]. Consequently, the development of oral small molecule agonists has emerged as an alternative approach, offering advantages such as improved patient compliance and bioavailability through oral administration [27–29]. These development have prompted further investigation into the elucidation of experimental structure of activate state GLP-1R-G_s complexes with or without orthosteric agonists [30–33], providing crucial insights into the activation mechanisms induced by different ligands.

Despite significant progress in understanding the activation mechanisms of GLP-1R, structural insights into ligand-induced modulation by balanced and biased agonists remain limited. In this study, we aim to provide molecular insights into the different functional agonists binding to GLP-1R. Specifically, we investigate three ligands Peptide 19, danuglipron, and CHU-128 using all-atom model molecular dynamics (MD) simulations (Table 1). They show distinct functional features: (1) Peptide 19, is an analog of gastric inhibitory polypeptide (GIP) exhibiting high potency for cAMP production at both GLP-1R and GIPR, but with notable partial agonism toward β-arrestin 2 recruitment [34]. (2) Danuglipron is a small molecule identified from high-throughput screening and shows potency comparable to GLP-1 the canonical GLP-1R peptide in *in vitro* studies, inducing both cAMP and β-arrestin signaling [28]. In a phase 2 trial, the administration of danuglipron improved metabolic function, although gastrointestinal side effects were observed [35]. (3) CHU-128 is a small molecule that exhibits strong bias toward the cAMP pathway and distinct binding mode profile compared to danuglipron [30]. All mentioned ligands induce unique conformational changes in the receptor, resulting in distinct packing arrangement of the 7TM helical bundle that influences the downstream protein sensitivity to the intracellular binding pocket [30,31].

Table 1. Information of simulated ligand.

Compounds	Danuglipron	CHU-128	Peptide 19
Chemical structure			
Molecular mass	555.6 g/mol	883.96 g/mol	4064 g/mol
Ligand type	Small Molecule	Small Molecule	38-residue Peptide
Activity type	Balanced	G protein biased	Balanced
Binding site	Orthosteric	Orthosteric	Orthosteric

Using all-atom MD simulations of the ligand-GLP-1R-G_s complex, we explore how orthosteric-bound binders induce the transduction of signals across the receptor to activate specific or impartial intracellular signaling pathways. Furthermore, we perform complementary simulations with peptide-free GLP-1R to gain deeper insights into the receptor conformational dynamics, particularly in the extracellular domain, which is critical for agonists binding and activation. Our simulations reveal that the ligand binding mode is directly correlated to the signaling pathway preference. Importantly, the limitations of small molecules in simultaneously managing the extracellular domain (ECD), transmembrane region, and core vestibule reflect their distinct advantages in conducting GLP-1R activation.

Materials and Methods

Complex Structure Preparation

To explore the structural dynamics of ligand-induced activation of the GLP-1R, we selected three ligand-receptor-G_s complexes, comprising danuglipron (PDB ID: 6X1A), CHU-128 (PDB ID: 6X19), or Peptide 19 (PDB ID: 7RTB) as ligands, and the G_s protein. Structurally unresolved residues, typically found in ECD-TM1 linker and ECL3 regions, were modeled using the Modeller program [36] and optimized with the Prepwizard module from the Schrodinger software suite [37]. To simulate the presence of G protein without overburdening the system, only the G_α subunit was

retained in the complex. For the MD simulation of the receptor alone, we remove the Peptide 19 and the G protein from the published structure of the ternary complex [31].

Molecular Dynamics Simulation Protocol

MD simulations were performed in a membrane-mimicking lipid bilayer system [38–40]. The lipid bilayer membrane was established using the CHARMM-GUI webserver [40] and distinct receptor complex structures were integrated in the lipid bilayer using the OPM webserver [41]. The lipid bilayer was composed of 1-palmitoyl-2-oleoylphosphatidylcholine (POPC). The receptor complex structure was embedded in a lipid bilayer of 240 lipids, hydrated to TIP3P water molecules with 0.15 M NaCl. All systems were simulated in GROMACS using CHARMM36m force field [42]. The systems were minimized with a 5,000-step energy minimization using the steepest descent algorithm and subjected to temperature equilibrating in the NPT ensemble at 310 K for 500 ps. For objective analysis, simulations were repeated three times with different initial velocities. In all holo-state structures used for simulations, the experimental structures of the G proteins and ligands were maintained, with additional restraints applied to the G protein backbone. For the ligand-free receptor structure, no structural restraints were applied. All replicas underwent 500 ns simulations to visualize large-scale motions.

Analysis of Simulated Structures

The MD data were analyzed using several methods to characterize the dynamic behavior of the receptor. Root-mean-square deviation (RMSD) and root-mean-square fluctuation (RMSF) were computed using the GROMACS program [42]. RMSD quantifies the deviation between the reference structure and the molecular trajectory, with the initial frame structure in the simulation typically used as the reference. RMSF evaluates the flexibility of individual atoms or residues throughout the simulation.

The DSSP method was employed to analyze hydrogen bonding patterns and the spatial arrangement of backbone atoms in a protein structure evaluating the angles between backbone atoms (C_α-N-C_α and N-C_α-C) and the distance between hydrogen bond donors and acceptors. Based on these hydrogen bonding patterns, DSSP classifies the protein secondary structures into four types including alpha helix, beta strand, turn, and loop [43].

The dynamic cross-correlation (DCC) method, implemented by Bio3D [44], was used to analyze coordinated movement between atoms in the MD trajectory. DCC provides insights into the collective behavior of residues in macromolecules, helping to identify functional dynamics and how different parts of the molecule move relative to one another. In MD simulations, atoms within a molecule continuously move, and DCC quantifies how these atomic displacements correlate over time. The DCC calculation is performed by computing the cross-correlation of atomic displacements over time.

The Residue Interaction Network Generator (RING) 4.0 [45] provides an advanced method for detecting and analyzing residue interactions, representing these interactions as a network with residues as nodes and their interaction information as edges, including the interaction type and interaction frequency.

Finally, the binding pocket volume was calculated using the POVME v3.0 tool [46], which characterizes the shape and flexibility of binding pockets within macromolecules. The software uses a cavity detection algorithm to evaluate the 3D spatial arrangement of atoms, identifying potential binding pockets based on their shape, size, and ligand accessibility. The center of the binding pocket was defined as the center of mass of the ligand for ligand-bound structures.

Results and Discussion

Distinct Binding Mode Led to Unique Signaling

To understand how the conformation, orientation and binding mode of ligands with distinct pharmacological profile influence the receptor's signaling pathway, we performed all-atom MD simulations for high-resolution structures of GLP-1R bound to different orthosteric ligands: (i) CHU-128 is a biased nonpeptide agonist, which induces a receptor conformation that favors G protein activation over β-arrestin recruitment signaling [30], (ii) danuglipron and (iii) Peptide 19 are a balanced nonpeptide and peptide agonist, respectively, which induce both cAMP production and β-arrestin recruitment pathways [30,31]. All these structures were simulated in complex with the G_s protein α-subunit ($G\alpha$) only (Table 2). To visualize the potential mechanism that promotes the receptor to transit from one set of conformational states populations to another one, we performed an additional ligand-free MD simulations using GLP-1R-Peptide 19 complex by removing the ligand and $G\alpha$. Three independent replicas' simulations of 500 ns duration were performed for each above-mentioned system.

Table 2. Summary of GLP-1R simulated system.

PDB	Simulation time (ns)	Resolution (Å)	Activity State	Ligand	Ligand Type	Downstream Protein
6X1A	3x500	2.50	Active	Danuglipron	Balanced agonist	G_s
6X19	3x500	2.10	Active	CHU-128	Biased agonist	G_s
7RTB	3x500	2.14	Active	Peptide 19	Balanced agonist	G_s
7RTB	3x500	2.14	Ligand-Free	-	-	-

(i) **The location of each ligand bound to the receptor**. Static structural analysis of ligand-receptor complexes indicates that danuglipron inserts deeply in the receptor's binding cavity closing the binding pocket, whereas CHU-128 adopts a planar binding pose above the helical transmembrane bundle, close to ECD, ECL1, and ECL2 liberating regions around TM6-TM7 [30] (Figure 1A). The position and binding modes of small molecule agonists involve different structural modulation associated to distinct pharmacology profiles. Peptide agonists are integrally buried with a longitudinal orientation in the receptor's binding vestibule, forming a helical structure within the transmembrane segments [47] (Figure 1). Either balanced or biased small molecule agonists form limited number of interactions with the core vestibule, suggesting that the extracellular interface plays a more critical role in signaling preferences than the buried region of the binding pocket. The contact with different transmembrane segments drives biased and balanced agonists to induce similar G-protein-bound conformations at the intracellular binding site, thereby regulating the binding affinity of downstream proteins. Effectively balanced agonists confer the receptor to a greater degree of conformational flexibility shifting the intracellular binding site from a large open to a more restrained state [48].

(ii) **Movement of TM region in small molecule-bound systems**. The binding position of danuglipron toward the upper region of TM6-ECL3-TM7 prompts this region to shift inward within the binding pocket promoting an overall contraction of the receptor structure [30] (Figure 1B). This contraction is crucial for mimicking the GLP-1-induced active receptor conformation. In contrast, no inward movement of these regions was observed for the CHU-128-bound structure, which instead shows a more extended conformation compared to peptide-bound structures. These distinct

structural changes contribute to the pharmacological activity of the receptor, which is driven by modulating the affinity for downstream signaling proteins [49].
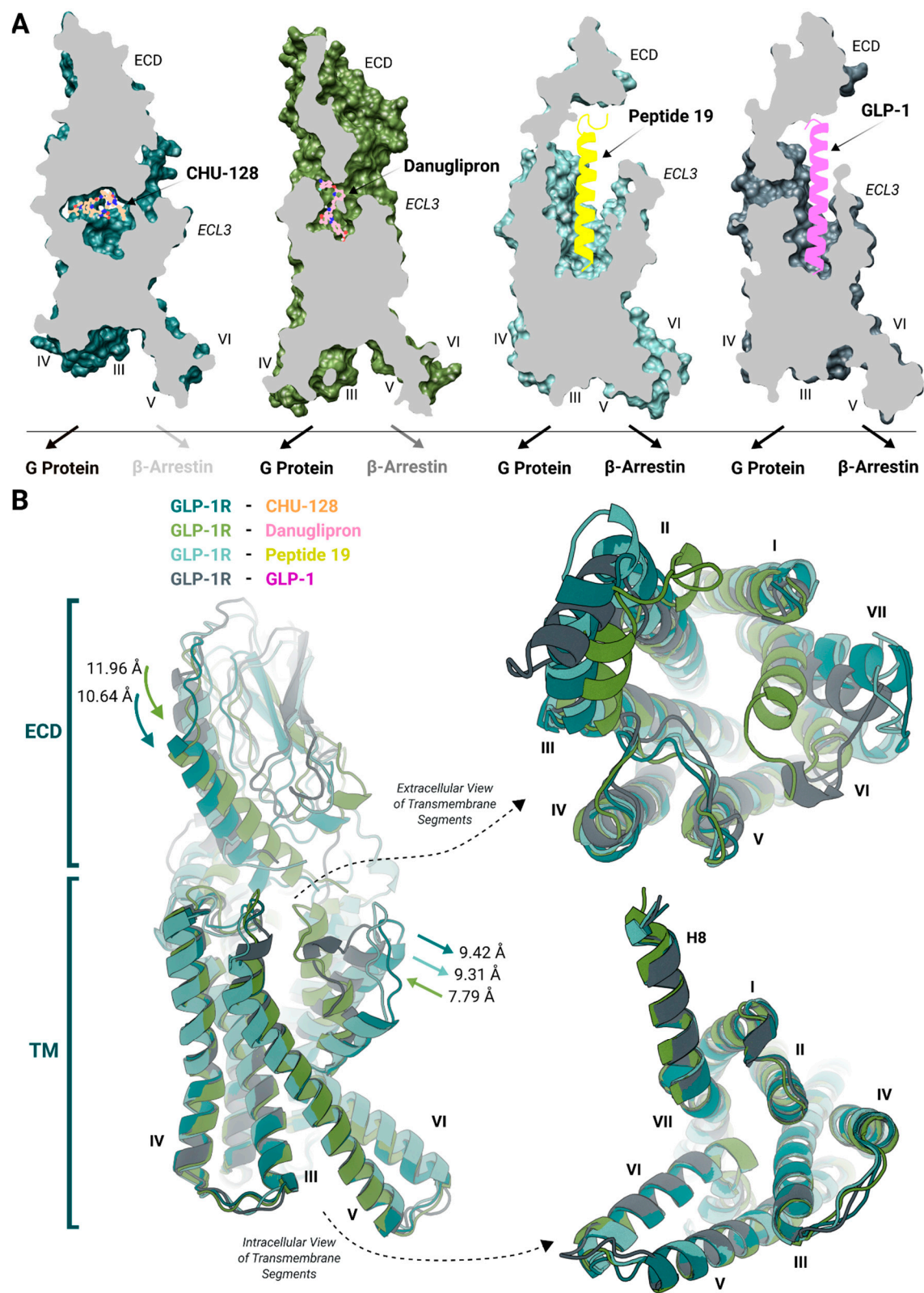
Figure 1. Structural comparison of GLP-1R bound to different agonists. A) Cross-section view of experimental GLP-1R-ligand-G$_s$ complex structures depicting CHU-128 (blue: receptor; orange: ligand), danuglipron (green: receptor; pink: ligand), Peptide 19 (cyan: receptor; yellow: ligand), and GLP-1 (black: receptor; purple: ligand) in their respective orthosteric binding pocket of GLP-1R. The transparency degree of downstream proteins reflects the relative potency and downstream signaling capacity of each ligand. B) Superposition of GLP-1R

structures comprising different bound ligands. The interface of the TM6-ECL3-TM7 region experiences significant displacement during receptor activation. Superposition of ligand-bound receptor structures reveals extracellular and intracellular conformational modulation, resulting in the formation of a similar intracellular cavity conformation among different types of ligands.

(iii) **Structural differences in extracellular regions**. There are noticeable differences in the structure of the receptor's extracellular regions upon binding to different ligands. Peptide 19 induced a 9.31 Å outward movement of TM6-ECL3-TM7 relative to the GLP-1-bound structure (Figure 1B). This shift may stabilize the binding of the ligand in the core vestibule [50]. While GLP-1 engages stable interactions with the core vestibule but dissociates rapidly, Peptide 19 forms transient interactions in this domain with sustained interactions with the ECD and extracellular region of transmembrane helices, contributing to more durable G protein activation [31]. Unlike typical class A binding mechanism, here the ECD plays a fundamental role in stabilizing the bound ligand [51]. Danuglipron induces a 7.79 Å inward movement of the TM6-ECL3-TM7 region, and the helix structure of ECD shifts by 11.96 Å into the binding pocket. This movement reinforces the helical bundle compaction. Similar to danuglipron, CHU-128 induces a 10.64 Å inward shift of the helix structure of the ECD. Actually, the conformational modulation of the ECD is highly dependent on the particular ligand structure. Interestingly, CHU-129 induces TM6-ECL3-TM7 shift comparable to that induced by Peptide 19. This region is associated with signaling pathways, highlighting the nuanced structural and functional differences between these ligands. In the structure of receptor bound to small molecule agonists like danuglipron, the ECD covers the binding pocket, reducing the distance of ECD to ECL2, ECL3, as well as ECL1 and transmembrane segments (Figure 1B), thereby the embedding of ECD substantially influences the signaling potency.

*Structural Dynamics of GLP-1R for Ligand-Bound and Ligand-Free Conditions*

To check how stable each structure is, we performed all atom MD simulations and summarized the systems in Table 2. In the simulations of the ligand-receptor complexes, the receptor backbone and most the ligand conformations remained stable throughout the trajectory (Figure 2A & S1), suggesting equilibrium binding for most of the simulated ligands. However, the danuglipron-bound complex exhibited notable conformational deviation of the ligand after 200 ns simulations (Figure S1 & S2). Different from other compounds, the danuglipron-bound structure did not preserve a thermodynamic stability in the binding pocket, in agreement with prior reports [30] (Figure 2A & C). This observation suggests that danuglipron maintains a relative flexible conformation, implying a faster dissociation rate.

In contrast, the ligand-free simulation revealed much larger receptor structural variations. In the absence of the peptide stabilization, the receptor showed a dramatically increased conformational distribution, especially in the ECD region (Figure 2A-B & S3). Unlike the stable conformation observed in replica 2, a larger conformational motion in replicas 1 and 3 cause the longitudinal ECD structure to cover upon the binding pocket, imitating that of a nonpeptide-bound state. Furthermore, the residual fluctuation plot revealed that increased fluctuations are typically associated with solvent-exposed regions, including the extracellular and intracellular loops and the ECD (Figure 2A, D & S1). Compared to the ligand-free state, the average fluctuation in the ECD domain are attenuated in the presence of bound ligand, suggesting that ligand engagement stabilizes this domain. These findings imply that the receptor performs transitions to an intermediate, partially active conformation upon ligand removal.

In addition, the dynamic cross correlation (DCC) analysis further illustrates residue-residue correlation during simulations (Figure 2D). In agonist-bound structures, the ECD exhibits strong positive correlations to ECL1 and ECL2, which are associated with selective downstream signaling. In the danuglipron-bound structure, additional correlation was observed between the ECD and the extracellular portion of TM7. This feature is absent in CHU-128- but present in Peptide 19-bound structures, highlighting potential involvement of TM1-TM7 coupling in regulating G protein-

independent signaling [52]. Interestingly, correlation between TM1-TM2 and TM5-TM6 was evident in danuglipron- and Peptide 19-bound systems but not in CHU-128. This intramolecular interaction network may underlie balanced G protein/β-arrestin signaling. In contrast, CHU-128 maintains structural flexibility within G protein signaling-associated segments. In the case of ligand-free structure, the ECD underwent pronounced rearrangement and showed minimal correlation to other domains, instead adopting a more energetically favorable conformation over the simulation time (Figure S3). Furthermore we observed enhanced correlated motions among ECL3, ICL3, TM5, and TM6, regions essential for signal transduction [53]. While the holo state exhibited more localized, direct residue-residue contacts within the transmembrane helices. The ligand-free state demonstrated overall increased flexibility and dynamic coupling, probably due to the absence of both the ligand and the G protein.
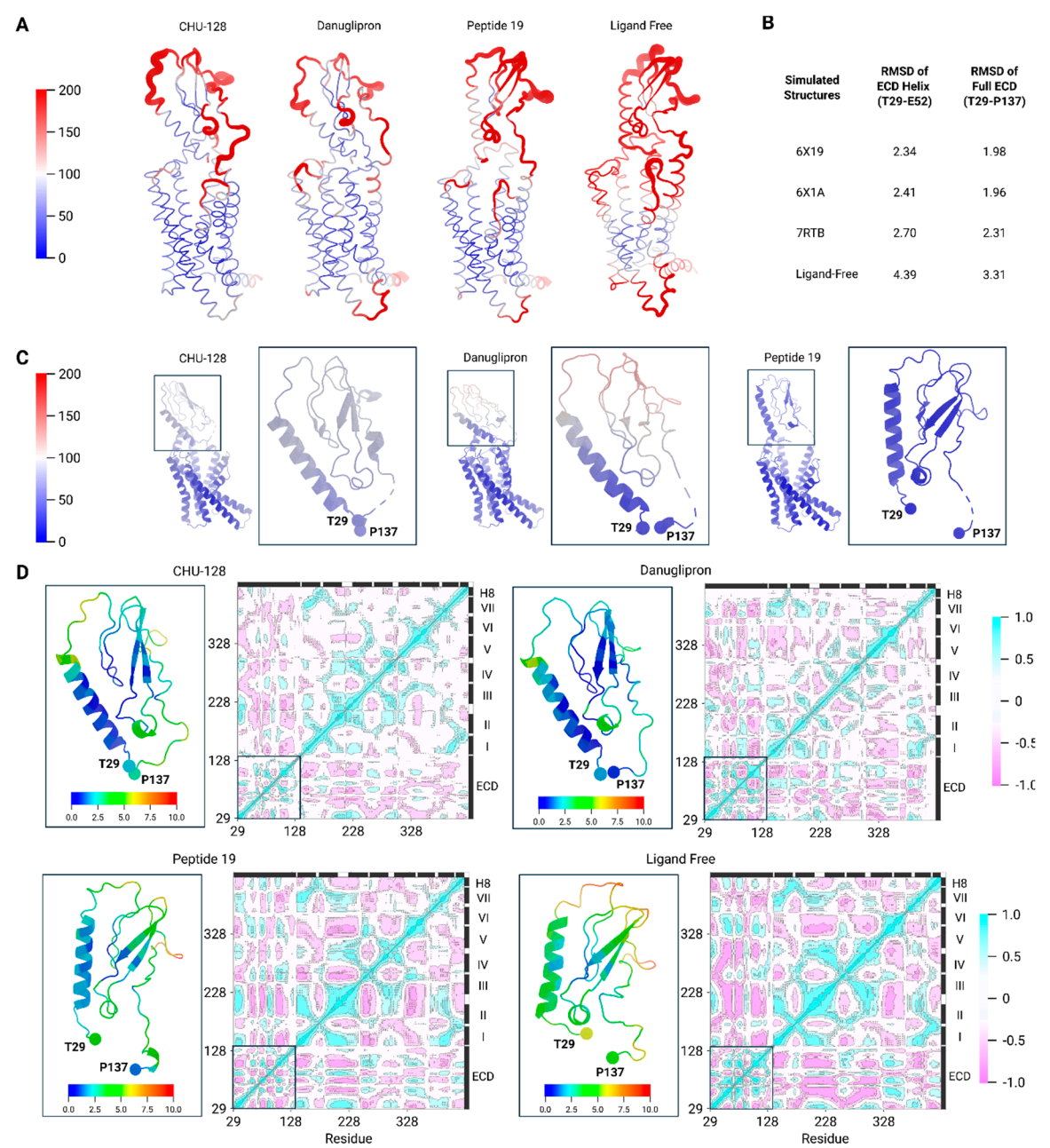

Figure 2. Residue-level dynamic cross correlation maps of GLP-R during MD simulations. A) Visualization of Cα backbone atom displacement in the ECD region, where blue and red represent low and high fluctuations. Representation of the receptor conformational motion in putty representation. The receptor structure is colored by B-factor values of GLP-1R estimated from the fluctuations of residues during simulation. B) RMSD of

ensemble simulation structures of GLP-1R-ligand complexes. C) Representation of experimental structures of ECD region colored by the experimentally determined B-factor. D) The dynamic cross correlation analysis reveals correlated motions among key structural domains of the receptor, including ECD, ECLs, ICLs, and TMs regions. The correlation coefficients range from -1 to 1, representing the complete negative correlation (blue) and complete positive correlation (red), respectively. The sequence of GLP-1R is color-coded by domain: ECD (yellow), ECLs (blue), ICLs (green), TMs (pink), and Helix 8 in (purple).

### Structural Plasticity of GLP-1R in the Holo State

To further establish the inherent dynamics of the receptor binding, we compared the simulated ligand-free structures to experimentally resolved ligand-free structures in complex with G proteins. Although these experimental structures have the capacity to engage in downstream signaling, the activation process shows reduced efficacy and frequency [32]. Our simulations captured near-native conformations of ligand-free structures (Figure 3), but two regions exhibited noticeable differences: the ECD and TM6-ECL3-TM7 segment. In the reference structure (initial frame), the helical structure of the ECD is oriented parallel to the transmembrane domain, however, in two simulation replicas, it is repositioned deeper in the orthosteric binding pocket (Figure S3). Notably, the ECD helix undergoes a pronounced shift of approximately 18 Å toward the ECL1 and ECL2 interface (Figure 3), a transitional conformation engaged that is rarely observed in computational approaches [54] or experimental structures [33]. This repositioning may result in transient ECD-transmembrane contacts that influence the receptor's conformational ensemble. Nevertheless, the resulting structure appears insufficiently stabilized to achieve full activation and remains less stable than agonist-bound conformations [33].
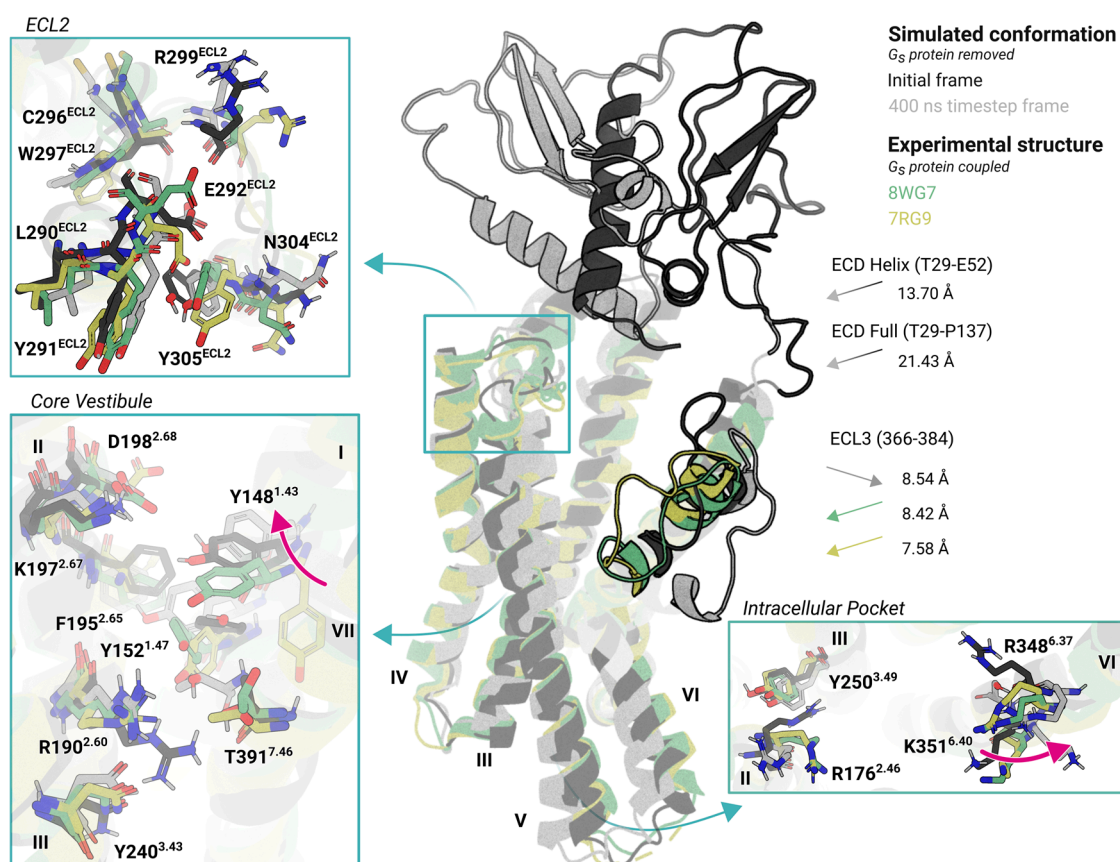
Figure 3. Structural superimposition of ligand-free conformations of GLP-1R. Experimental (yellow: PDB ID 7RG9; green: PDB ID 8WG7) and simulated ligand-free structures (black: initial simulation frame; gray: last simulation frame) are aligned. The superimposed models highlight conformational transitions, particularly in ECL2, the G protein binding pocket, and the core vestibule. Key residue orientations in the simulated structures

show notable convergence toward experimentally observed conformations. The RMSDs were computed between the C_α atoms of corresponding residues of the two structures, revealing substantial structural variability in the ECD and ECL3 regions.

Binding Pocket Variants Upon Danuglipron, CHU-128, and Peptide 19 Binding

In the presence of ligand, the ECD is stabilizing the orthosteric binding pocket and forms multiple interactions with the ligand throughout the simulations. In small molecule-bound structures, residue W33[ECD] engages in π-stacking interactions with the indole group of CHU-128 and pyridine ring of danuglipron along the simulations. In addition, both ligands form hydrogen bonds with R299[ECL2], anchoring the ligand to the extracellular loop 2. Despite these shared interactions, CHU-128 and danuglipron exhibit distinct binding feature at the ECL3 and TM7 interface (Figure 4A-B). The acid carboxylic group of danuglipron forms polar interactions with ECL3 (R376[ECL3]) and TM7 (R380[7.35]), reinforcing a closed conformation of the TM6-ECL3-TM7 region. However, the dimethylfluorobenzene group of CHU-128 creates a hydrophobic environment that pushes polar residues of TM6-ECL3-TM7 away, thereby expanding the binding cavity.

Intriguingly, the Peptide 19 also interacts with TM7 and ECL2 but still induces an opened binding pocket conformation (Figure 4C). This difference arises because Peptide 19 is engaged in extensive interactions with the receptor core, effectively acting as a semi-transmembrane helix during activation. In agreement with previously reports [50], Peptide 19 is stabilized through sustained interactions between the C-terminal region of the peptide and the ECD domain. Although, Peptide 19 shares high sequence similarity with endogenous GLP-1, a tyrosine in Peptide 19 instead of histidine at the N-terminal position (residue 1) introduces steric hindrance with Q234[3.33], redirecting its orientation toward TM5. The tyrosine transiently interacts with R310[5.44], disrupting the contact with the ECL3 region and liberating the TM6-ECL3-TM7. During the simulations, the peptide maintained stable electrostatic interactions with E387[7.42], limiting the degree of TM7 displacement observed in ligand-free structure simulations. These interactions contribute to the peptide's consistent positioning within the orthosteric site and its ability to regulate transmembrane packing, supporting both G protein-dependent and -independent signaling pathways.
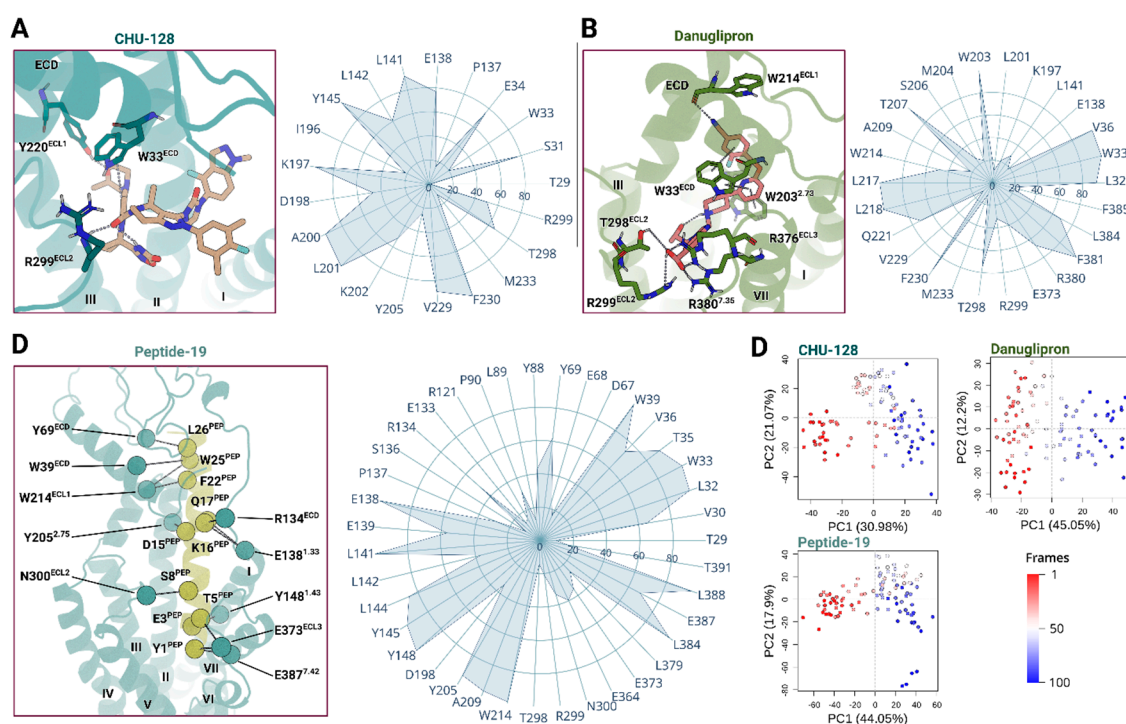
Figure 4. Distinct binding modes of GLP-1R agonists. Distinct properties of the binding pocket of GLP-1R in complex with three agonists obtained from MD simulations: A) CHU-128 (blue: receptor; beige: ligand), B)

danuglipron (green: receptor; red: ligand), C) Peptide 19 (cyan: receptor; yellow: ligand). Each ligand adopts a unique binding pose within the orthosteric site. The receptor–ligand contact networks remain stable throughout the MD simulations, indicating sustained interactions that support their distinct pharmacological profiles. D) The principal component of residues contribution in structural motions. PC1 captures 31%, 45%, and 44% of total variance in trajectory conformation set of CHU-128-, danuglipron-, and Peptide 19-bound complexes, respectively. Conformations are colored from red to blue in order of simulation time.

Signal Transduction Associated with Distinct Types of Ligand Binding

Ligand Recognition and Binding via the Extracellular Domain

Previous studies have emphasized the important role of W33[ECD] for the ligand recognition and binding [29,55] (Figure 4). However, the specific chemical architecture of each ligand induces distinct extracellular rearrangements, which are followed by conformational changes in TM1 and TM7 (Figure 5). The binding mode of danuglipron promotes a compact conformation by stabilizing the ECD toward TM1 and TM7, leading S31[ECD] to form a hydrogen bond network with E138[1.33] and T378[7.33], thereby repositioning TM7 closer to TM1 and effectively enclosing the binding pocket. In contrast, the ligands CHU-128 and Peptide 19 hinder this convergence by acting as steric barriers. This results in an increased distance between E138[1.33] and T378[7.33] (~13.6 Å of C_α of residues), preventing closure of the TM1-TM7 interface.

CHU-128 displaces the ECD toward ECL2, forming strong and stable polar interaction with G295[ECL2] and T298[ECL2] (Figure 5), while danuglipron and Peptide 19 show either very transient or no hydrogen bonds at this interface. Stabilization of the ECD is further reached by Q221[ECL1], which forms persistent hydrogen bonds with Q37[ECD] and R40[ECD] (Figure 5). Interestingly, ECL1 interacts preferentially with Q37[ECD] over R40[ECD] in CHU-128 bound and ligand-free structures, but favors interaction of R40[ECD] with ECL1 in danuglipron- and Peptide 19-bound structures. This may be associated with balanced agonists that pull away the ECD from ECL1-ECL2, thus only the longer side chain of R40[ECD] maintains the contact with ECL1. Overall, these ligand-receptor interaction patterns define the orientation and spatial dynamics of the ECD in the binding pocket during MD simulations. Notably, the binding mode of CHU-128 and danuglipron are typical for G protein-biased and balanced nonpeptide agonists, respectively, inducing the ECD toward either ECL2 or TM1-TM7 regions. Despite CHU-128 induces a more open binding pocket, which intuitively is associated with rapid ligand dissociation, cell-based experiments report a higher binding affinity for CHU-128 compared to danuglipron [30]. Thus, the dissociation kinetics may not only be governed by transmembrane rearrangements but also by the hydrophobic character of the ligand, which affects retention within the solvent-exposed binding pocket. Danuglipron, by enclosing the binding pocket, gain increased binding energy to stabilize structure packing. As class B GPCRs typically accommodate large peptide ligands via expanded orthosteric binding pockets, the evolutionary design includes an extended N-terminal domain to realize high-affinity binding [56].

Signal Transduction along the Transmembrane Domain

Within the core vestibule, key residues in TM1, TM2, TM3, and TM7 contribute to helical packing. In the ligand-free simulated structures, a transient π-stacking network forms among Y148[1.43], Y152[1.47], and F195[2.58]. This network occasionally extends to Y145[1.40], K197[2.67], D198[2.68], and K202[2.72] in the holo state structure (Figure 5), enhancing TM1 packing with other TM regions. However, in ligand-free structures, Y145[1.40] shift outward, disrupting the interaction with TM1-TM2 contact and leading to expansion of the TM6-ECL3-TM7 interface, enlarging the open conformation. These rearrangements lead to the greater dynamics within the TM helical bundle and extends the binding pocket. In contrast, ligand-bound structures exhibit reduced transmembrane flexibility, stabilizing an active-like conformation. In Peptide 19-bound structures, Y145[1.40] interacts with K202[2.72] mediated by Y10[PEP], reinforcing TM1-TM2 association (Figure 4). For small molecules, the receptor forms consistently direct interactions between D198[2.68] with Y145[1.40] and Y148[1.43] in danuglipron-bound

structures and supplementary interactions K202[2.72] and Y145[1.40] for CHU-128-bound structures, but the functional role of Y148[1.43] and Y152[1.47] differ in the core vestibule. Specifically, in danuglipron-bound structures, Y152[1.47] forms hydrogen bonds with T391[7.46], pulling TM1 toward TM7 and priming the receptor for β-arrestin-dependent signaling. In case of Peptide 19, the peptide bridges TM1 and TM7, stabilizing the core vestibule and supporting both G protein- and β-arrestin-dependent pathways. In contrast, the simulations of CHU-128-bound and ligand-free structures exhibit disengagement of Y152[1.47] from TM7, implying that these configurations are less favorable TM helical packing. Furthermore, Y152[1.47] often shifts from the core to the membrane periphery, suggesting a functional role during activation.

In addition, TM6 is integrally involved in the TM helical packing. An approximate 90° kink of TM6 is a hallmark of class B GPCR activation, distinguishing it from class A GPCRs. In our simulations, the kink was present in the active and in the ligand-free state, unless external stimuli forcing TM6 to engage a less kinked conformation. In all simulated structures, we observe that ligand-free structures exhibit the largest opening, where the kink angle deviation is comparable to that of CHU-128-bound structures (Figure 6). This suggests that the TM6 kink is adjusted to optimally bind large peptide ligands that modulate the downstream signaling. In the basal state, the TM6 conformation is preferentially shaped to the association of the G protein. Binding of danuglipron induced a straighter TM6 helix conformation, with kink angles fluctuating between 100-125°, still approximately 20-30° greater than those found in CHU-128-bound structures (Figure 6). This conformational bias is supported by strong polar interactions across the binding pocket, such as between E34[ECD]-T378[7.33], R299[ECL2]-R380[7.45], R299[ECL2]-E373[ECL3], R310[5.44]-E373[ECL3], S301[ECL2]-E376[ECL3], R190[2.60]-E364[6.53], which constrain TM6 straightening (Figure 5 & S3).

Features of the Intracellular Binding Domain

To stabilize the active state, residue Y402[7.53] interacts with R176[2.39], E247[3.46], and T355[6.39] enhancing the stability further by engaging Y359 of the G protein (Figure 6B & S5). R176[2.46] performs a transition from an open to a closed locked state through a shift toward the H8 and the Y402[7.53] interacts with T355[2.48], maintaining the TM6 in a kinked conformation. During the deactivation process, the TM6 undergoes exploratory shifts and rotations toward the intracellular binding site, releasing Y402[7.53] which then orients toward the core vestibule, forming polar interaction with R247[3.50] and T353[6.37] (Figure 6A). Residue R176[2.46] further reinforces the closed conformation by forming a hydrogen bond network with N406[8.46], E408[8.48], and R348[6.37], thereby firmly closing the structure. In the active state, residues N406[8.46] and E408[8.48] form transient interaction with the G protein, and E408[8.48] is believed to initiate the G protein binding [57]. In the absence of the G protein, residue N406[8.48] forms an internal interaction with the backbone of Y402[7.53], suggesting that the N-terminal of H8 plays a critical role in recognizing G protein and maintaining the structural stability.

Structural analysis of the intracellular binding pocket reveals a variation in the binding mode of the G protein when danuglipron is bound to the receptor, as compared to other receptor-ligand complexes (Figure 6B & S6). During simulation, the G protein in the danuglipron-bound structure shifts closer to the TM3-TM5-TM6 regions, resulting in detachment from ICL2 and H8. This movement suggests that danuglipron induces a distinct conformation of the receptor, which is less stable or less tightly associated with the G protein than other ligands. In contrast, CHU-128 and Peptide 19-bound structures maintain G-protein interactions with both the receptor's TM3-TM5-TM6 regions and the intracellular loop (ICL2 and H8), likely stabilizing the receptor-G protein complex more effectively and for a longer duration. This distinct variation in the binding mode may explain why danuglipron exhibits lower activity potency than CHU-128 [34], despite both ligands interacting with the receptor and initiating G protein signaling. Thus, differences in ligand binding modes likely influence the efficacy and potency of G protein activation.

Unlike class A GPCRs, GLP-1R lacks the conserved NPxxY[7.53] motif at the intracellular region of TM7, which is crucial for ligand-induced conformational changes [58]. In class A GPCRs, the asparagine in this motif stabilizes the active/inactive state and is tightly involved in receptor

signaling. However, in GLP-1R, the positions 7.49 and 7.50 contain small hydrophobic residues. Furthermore, GLP-1R does possess the conserved Y402[7.53] residue, which forms direct T-shaped interactions with the tyrosine at the C-terminal end of G protein. These observations suggest that the 7.49 and 7.50 positions play a lesser important role in receptor activation, implying that peptide hormone ligand-induced receptors may have a distinct activation mechanism [59].
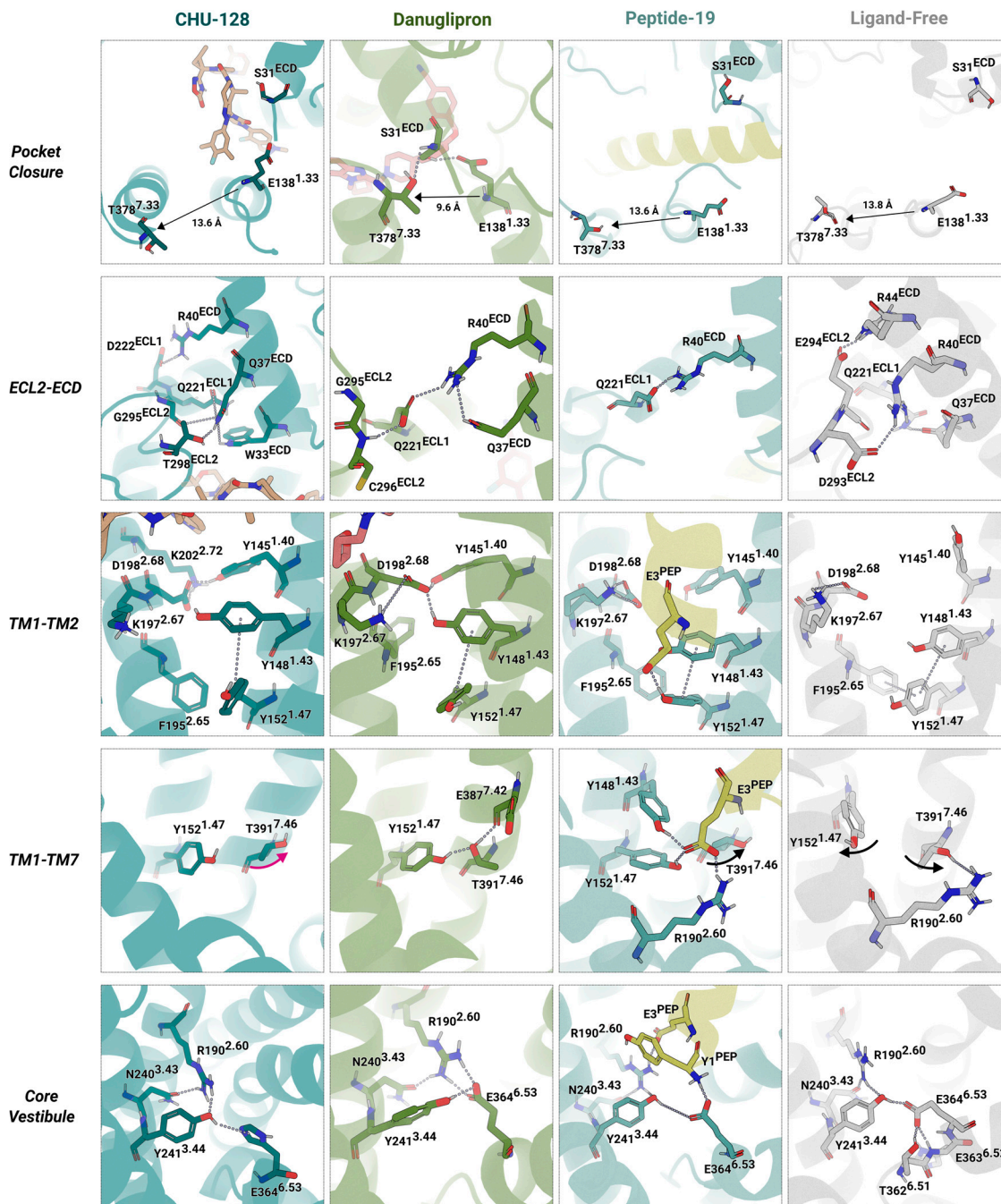

Figure 5. Residue interaction networks of GLP-1R at different ligand binding conditions. Structural configuration of GLP-1R bound to CHU-128, danuglipron, Peptide 19, and ligand-free states are shown. The packing of the receptor is intrinsically mediated by the specific agonist. Danuglipron requires harmonic engagement of the TM6–ECL3–TM7 region to mimic the signal transduction observed in peptide agonists. Peptide 19 also involves this region in receptor activation. In contrast, CHU-128-bound and ligand-free structures exhibit a less compact arrangement of the seven transmembrane helices.

Biased Agonism and Receptor Signaling Mechanisms

Inferring β-Arrestin-Bound to GLP-1R via Structural Comparison with Related Class B1 GPCRs

Interestingly, experimental structures of ligand-free GLP-1R maintain an open conformation of the intracellular binding region (Figure 6a), denoting the receptor to adopt G protein-preferred conformation [33]. The extracellular portions of TM1, TM6, and TM7 shift outward in the ligand-free state in contrast to the inward movements observed upon peptide binding. The CHU-128-bound and ligand-free GLP-1R structures exhibit similar conformations of the receptor in the extracellular regions, preferentially activating the cAMP accumulation pathway. In this context, the packing between TM1, TM2, and TM7 at the intracellular side is critical for β-arrestin recognition and binding (Figure S4). Interestingly, simulation of danuglipron- and Peptide 19-bound receptor complexes displayed that R176$^{2.46}$ rotates toward the H8 of GLP-1R, forming strong polar interaction in inactive receptor state (Figure 6B). We speculate that the rotation of the arginine is key factor for the transition of the G-protein-preferred to the β-arrestin-preferred conformation. Other β-arrestin-bound structures provide additional clarification into the biased signaling mechanism of GLP-1R. The potential conformation of the GLP-1R-β-arrestin complex was deduced from the experimental structure of another glucagon receptor (GCGR)-β-arrestin complex, because GCGR is one of the few classes B1 GPCRs for which structures in complex with β-arrestin are available. In the structures of GCGR-β-arrestin complexes in either glucagon-bound or ligand-free states, TM5 and TM6 exhibit a similar arrangement as found in the inactive state of GLP-1R (Figure 6A & S4). This suggests that GLP-1R potentially "dekinks" TM6 during β-arrestin binding (Figure S4). Furthermore, the arginine (2.47) interacts with E$^{8.49}$, limiting the intracellular binding pocket to interact the G protein (Figure 6A). Consequently, balanced agonists compact the overall TM helical bundle structure by shifting TM5, TM6, and TM7 inward, which means that intermediate states are transient ensembles capable of transitioning from active-like to inactive-like conformations.

Although the ligand-free structure allows the receptor to explore a broader conformational landscape, unbiased MD simulations have to reach full transition from a G-protein-adapted conformation to a β-arrestin-adapted state, where the receptor must adopt an inactive-like conformation that promotes β-arrestin binding (Figure S4) The simulated ligand-free structures remain poised to engage G$_s$ protein binding, due to the difficulty to reach the dekinked, straight TM6. In contrast, the ligand-free experimental structures display higher degree of expansion, leading to reduced packing between TM1, TM6, and TM7 to the rest of the structure, and thereby promoting a more frequently opened conformation in the intracellular binding pocket. During the simulations, the hydrogen bonding between R190$^{2.53}$ and T391$^{7.41}$ is disrupted due to the outward displacement of TM7, accompanied by outward shifts of Y148$^{1.43}$ and D198$^{2.68}$ (Figure 3). These results support that GLP-1R can achieve basal activation of cAMP signaling pathways in the absence of bound ligand, while G protein-independent pathways may require further structural stabilization. The unoccupied intracellular region also permits transient side-chain rearrangements that may interfere with stable effector binding.
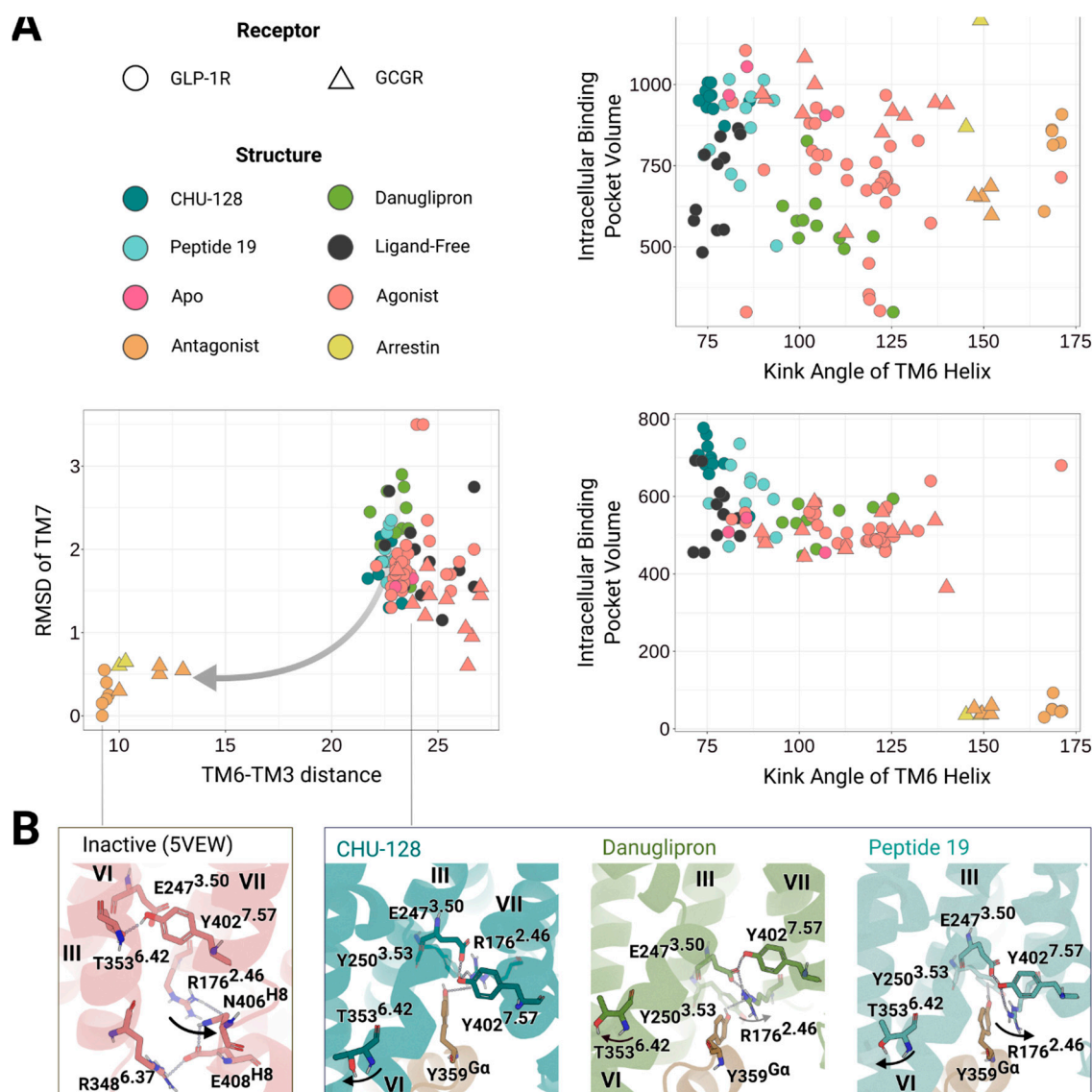
Figure 6. Conformational adaption of the intracellular signaling pocket of GLP-1R upon binding of different ligands. A) Structural comparison between the G-protein-bound active state and the inactive state of GLP-1R. The RMSD of TM7 (Å) is measured using C_α atoms of residues 7.49 and 7.54, with reference to the inactive state structure (5VEW). The distance (Å) between TM3 and TM6 is measured between residues 3.50 and 6.34. The volumes of the intracellular and extracellular binding sites ($Å^3$) are calculated with POVME. B) Intramolecular interactions of the core vestibule. Different residues are involved in the structural states through rotation and kinking of TM6.

Promising Pharmacokinetics of Biased Agonists

Balanced agonists typically induce a receptor conformation similar to that of the endogenous GLP-1-bound structure, prerequisite for activation of both G protein and β-arrestin signaling pathways. In contrast, G-protein biased small molecule agonists, binding at the extracellular interface, promote receptor conformations that preferentially activate G protein signaling while attenuating β-arrestin recruitment [30]. Similar to CHU-128-bound structures, exendin-P5, a G protein-biased ligand, primarily interacts with the TM4-TM5 regions and to lesser extent with TM1-TM7, supporting the hypothesis that signaling pathways are tightly linked to ligand binding orientation within the transmembrane regions [60]. Thus, G protein-biased agonists can disrupt interactions between TM1-TM7, which are associated with downstream protein coupling [61], thereby attenuating β-arrestin engagement.

G protein-biased GLP-1R full agonists, such as P5 and PX17, have been shown to improve glucose control and facilitate weight loss without significant appetite suppression or nausea, which could be attributed to alternative signaling pathways [18,62]. These agonists enhance anti-hyperglycemic efficacy by limiting the structural changes of TM6-ECL3-TM7 and TM1 in GLP-1R, reducing receptor desensitization and internalization [18,30,63]. The binding of CHU-128 induces a significant rearrangement within the binding pocket of GLP-1R and creates a large opening in the ECL3, which leads to the weak packing of TM5-TM6. In contrast, danuglipron stabilizes the binding pocket by pulling ECL3 closer to the binding pocket, which unexpectedly attenuates the activity potency of the ligand. Biased agonists that induce prolonged activation enhance the hypoglycemic effect and reducing side effects from the β-arrestin signaling pathway. Another promising approach to enhance the therapeutic curation of metabolic disease is the development of multi-target agonists, such as Peptide 19 and tirzepatide, which improve T2D treatment by combining the therapeutic effects of both GLP-1 and GIP receptors.

Conclusion

In summary, this work provides detailed molecular insights into different types of agonists coupling to GLP-1R. We have used structure-based MD simulations to resolve G protein-biased and balanced agonist induced signaling for GLP-1R. The G-protein biased compound CHU-128 stabilizes the receptor structure in active state by maintaining large open conformation of the receptor's ligand binding pocket. In contrast, the binding of danuglipron assembles extracellular portions of the transmembrane helices, which may require a higher energy barrier to maintain closed conformation of the binding pocket [64]. Notably, a change of the kink angle of 20-30° in the TM6 helix which shifts the extracellular region of TM6 toward the binding pocket is essential to cope with the energy barrier required for prolonged activation [64]. In addition, a limitation of using small molecule ligands as potential drugs is their inability to simultaneously modulate the extracellular domain, the extracellular parts of transmembrane domains and the core TM vestibule. However, they can still mimic the activity of peptide agonists, offering alternative assets to enhance the oral bioavailability and metabolic stability of GLP-1R targeting drugs. Our MD simulations showed that balanced agonist-bound structures tend to adapt a G-protein-independent signaling conformation in the intracellular binding region. As class B receptors, GLP-1R can adopt similar inactive-like conformation as found for GCGR to engage β-arrestin, but may not reach the full β-arrestin active state of the receptor in the absence of particular agonists.

Abbreviations

GLP-1R, glucagon-like peptide 1 receptor; SM, small molecule; MD: molecular dynamics; GPCR, G protein-coupled receptor; T2B: type 2 diabetes; ECD, extracellular domain; GLP-1RA, GLP-1R agonist; RMSD: root mean square deviation; RMSF, root mean square fluctuation; DCC, dynamic cross-correlation; RING; Residue Interaction Network Generator; H8, Helix 8; GCGR: glucagon receptor.

References

1. Hauser, A.S.; Kooistra, A.J.; Munk, C.; Heydenreich, F.M.; Veprintsev, D.B.; Bouvier, M.; Babu, M.M.; Gloriam, D.E. GPCR activation mechanisms across classes and macro/microscales. *Nat Struct Mol Biol* **2021**, *28*, 879–888, doi:10.1038/s41594-021-00674-7.

2. Li, H.; Sun, X.; Cui, W.; Xu, M.; Dong, J.; Ekundayo, B.E.; Ni, D.; Rao, Z.; Guo, L.; Stahlberg, H.; et al. Computational drug development for membrane protein targets. *Nat Biotechnol* **2024**, *42*, 229–242, doi:10.1038/s41587-023-01987-2.

3. Anantakrishnan, S.; Naganathan, A.N. Thermodynamic architecture and conformational plasticity of GPCRs. *Nat Commun* **2023**, *14*, 128, doi:10.1038/s41467-023-35790-z.

4. He, X.; Li, J.; Shen, S.; Xu, H.E. AlphaFold3 versus experimental structures: assessment of the accuracy in ligand-bound G protein-coupled receptors. *Acta Pharmacol Sin* **2025**, *46*, 1111–1122, doi:10.1038/s41401-024-01429-y.

5. McLean, B.A.; Wong, C.K.; Campbell, J.E.; Hodson, D.J.; Trapp, S.; Drucker, D.J. Revisiting the Complexity of GLP-1 Action from Sites of Synthesis to Receptor Activation. *Endocrine Reviews* **2021**, *42*, 101–132, doi:10.1210/endrev/bnaa032.

6. Zheng, Z.; Zong, Y.; Ma, Y.; Tian, Y.; Pang, Y.; Zhang, C.; Gao, J. Glucagon-like peptide-1 receptor: mechanisms and advances in therapy. *Sig Transduct Target Ther* **2024**, *9*, 1–29, doi:10.1038/s41392-024-01931-z.

7. Nauck, M.A.; Quast, D.R.; Wefers, J.; Meier, J.J. GLP-1 receptor agonists in the treatment of type 2 diabetes – state-of-the-art. *Mol Metab* **2020**, *46*, 101102, doi:10.1016/j.molmet.2020.101102.

8. Wang, J.-Y.; Wang, Q.-W.; Yang, X.-Y.; Yang, W.; Li, D.-R.; Jin, J.-Y.; Zhang, H.-C.; Zhang, X.-F. GLP–1 receptor agonists for the treatment of obesity: Role as a promising approach. *Front Endocrinol (Lausanne)* **2023**, *14*, 1085799, doi:10.3389/fendo.2023.1085799.

9. Zhang, X.; Cao, C.; Zheng, F.; Liu, C.; Tian, X. Therapeutic Potential of GLP-1 Receptor Agonists in Diabetes and Cardiovascular Disease: Mechanisms and Clinical Implications. *Cardiovasc Drugs Ther* **2025**, doi:10.1007/s10557-025-07670-9.

10. Vetrugno, L.; Deana, C.; Da Porto, A.; Boero, E.; Bellini, V.; Biasucci, D.G.; Bignami, E.G. A narrative review of glucagon-like peptide-1 receptor agonists prior to deep sedation or general anesthesia. *J Anesth Analg Crit Care* **2025**, *5*, 1–10, doi:10.1186/s44158-025-00237-y.

11. Andreasen, C.R.; Andersen, A.; Knop, F.K.; Vilsbøll, T. How glucagon-like peptide 1 receptor agonists work. *Endocr Connect* **2021**, *10*, R200–R212, doi:10.1530/EC-21-0130.

12. Zhao, X.; Wang, M.; Wen, Z.; Lu, Z.; Cui, L.; Fu, C.; Xue, H.; Liu, Y.; Zhang, Y. GLP-1 Receptor Agonists: Beyond Their Pancreatic Effects. *Front Endocrinol (Lausanne)* **2021**, *12*, 721135, doi:10.3389/fendo.2021.721135.

13. Gilbert, M.P.; Pratley, R.E. GLP-1 Analogs and DPP-4 Inhibitors in Type 2 Diabetes Therapy: Review of Head-to-Head Clinical Trials. *Front Endocrinol (Lausanne)* **2020**, *11*, 178, doi:10.3389/fendo.2020.00178.

14. Monti, G.; Gomes Moreira, D.; Richner, M.; Mutsaers, H.A.M.; Ferreira, N.; Jan, A. GLP-1 Receptor Agonists in Neurodegeneration: Neurovascular Unit in the Spotlight. *Cells* **2022**, *11*, 2023, doi:10.3390/cells11132023.

15. Ferhatbegović, L.; Mršić, D.; Macić-Džanković, A. The benefits of GLP1 receptors in cardiovascular diseases. *Front Clin Diabetes Healthc* **2023**, *4*, 1293926, doi:10.3389/fcdhc.2023.1293926.

16. Nevola, R.; Epifani, R.; Imbriani, S.; Tortorella, G.; Aprea, C.; Galiero, R.; Rinaldi, L.; Marfella, R.; Sasso, F.C. GLP-1 Receptor Agonists in Non-Alcoholic Fatty Liver Disease: Current Evidence and Future Perspectives. *Int J Mol Sci* **2023**, *24*, 1703, doi:10.3390/ijms24021703.

17. Zaïmia, N.; Obeid, J.; Varrault, A.; Sabatier, J.; Broca, C.; Gilon, P.; Costes, S.; Bertrand, G.; Ravier, M.A. GLP-1 and GIP receptors signal through distinct β-arrestin 2-dependent pathways to regulate pancreatic β cell function. *Cell Reports* **2023**, *42*, 113326, doi:10.1016/j.celrep.2023.113326.

18. Jones, B. The therapeutic potential of GLP-1 receptor biased agonism. *British Journal of Pharmacology* **2022**, *179*, 492–510, doi:10.1111/bph.15497.

19. Jones, B.; McGlone, E.R.; Fang, Z.; Pickford, P.; Corrêa, I.R.; Oishi, A.; Jockers, R.; Inoue, A.; Kumar, S.; Görlitz, F.; et al. Genetic and biased agonist-mediated reductions in β-arrestin recruitment prolong cAMP signaling at glucagon family receptors. *J Biol Chem* **2020**, *296*, 100133, doi:10.1074/jbc.RA120.016334.

20. Lucey, M.; Pickford, P.; Bitsi, S.; Minnion, J.; Ungewiss, J.; Schoeneberg, K.; Rutter, G.A.; Bloom, S.R.; Tomas, A.; Jones, B. Disconnect between signalling potency and in vivo efficacy of pharmacokinetically optimised biased glucagon-like peptide-1 receptor agonists. *Mol Metab* **2020**, *37*, 100991, doi:10.1016/j.molmet.2020.100991.

21. Guo, W.; Xu, Z.; Zou, H.; Li, F.; Li, Y.; Feng, J.; Zhu, Z.; Zheng, Q.; Zhu, R.; Wang, B.; et al. Discovery of ecnoglutide – A novel, long-acting, cAMP-biased glucagon-like peptide-1 (GLP-1) analog. *Molecular Metabolism* **2023**, *75*, 101762, doi:10.1016/j.molmet.2023.101762.

22. Marzook, A.; Tomas, A.; Jones, B. The Interplay of Glucagon-Like Peptide-1 Receptor Trafficking and Signalling in Pancreatic Beta Cells. *Front. Endocrinol.* **2021**, *12*, doi:10.3389/fendo.2021.678055.

23. Kassem, S.; Khalaila, B.; Stein, N.; Saliba, W.; Zaina, A. Efficacy, adherence and persistence of various glucagon-like peptide-1 agonists: nationwide real-life data. *Diabetes, Obesity and Metabolism* **2024**, *26*, 4646–4652, doi:10.1111/dom.15828.

24. Ceron, E.L.; Reddy, S.D.; Kattamuri, L.; Muvva, D.M.; Chozet, L.; Bright, T. Current Insights, Advantages and Challenges of Small Molecule Glucagon-like Peptide 1 Receptor Agonists: A Scoping Review. *Brown Hospital Medicine* **2025**, *4*, 23–36, doi:10.56305/001c.132255.

25. Drucker, D.J. GLP-1-based therapies for diabetes, obesity and beyond. *Nat Rev Drug Discov* **2025**, 1–20, doi:10.1038/s41573-025-01183-8.

26. He, X.; Zhao, W.; Li, P.; Zhang, Y.; Li, G.; Su, H.; Lu, B.; Pang, Z. Research progress of GLP-1RAs in the treatment of type 2 diabetes mellitus. *Front. Pharmacol.* **2025**, *15*, 1483792, doi:10.3389/fphar.2024.1483792.

27. Zhang, H.; Wu, T.; Wu, Y.; Peng, Y.; Wei, X.; Lu, T.; Jiao, Y. Binding sites and design strategies for small molecule GLP-1R agonists. *European Journal of Medicinal Chemistry* **2024**, *275*, 116632, doi:10.1016/j.ejmech.2024.116632.

28. Griffith, D.A.; Edmonds, D.J.; Fortin, J.-P.; Kalgutkar, A.S.; Kuzmiski, J.B.; Loria, P.M.; Saxena, A.R.; Bagley, S.W.; Buckeridge, C.; Curto, J.M.; et al. A Small-Molecule Oral Agonist of the Human Glucagon-like Peptide-1 Receptor. *J. Med. Chem.* **2022**, *65*, 8208–8226, doi:10.1021/acs.jmedchem.1c01856.

29. Kawai, T.; Sun, B.; Yoshino, H.; Feng, D.; Suzuki, Y.; Fukazawa, M.; Nagao, S.; Wainscott, D.B.; Showalter, A.D.; Droz, B.A.; et al. Structural basis for GLP-1 receptor activation by LY3502970, an orally active nonpeptide agonist. *Proc Natl Acad Sci U S A* **2020**, *117*, 29959–29967, doi:10.1073/pnas.2014879117.

30. Zhang, X.; Belousoff, M.J.; Zhao, P.; Kooistra, A.J.; Truong, T.T.; Ang, S.Y.; Underwood, C.R.; Egebjerg, T.; Šenel, P.; Stewart, G.D.; et al. Differential GLP-1R Binding and Activation by Peptide and Non-peptide Agonists. *Molecular Cell* **2020**, *80*, 485-500.e7, doi:10.1016/j.molcel.2020.09.020.

31. Johnson, R.M.; Zhang, X.; Piper, S.J.; Nettleton, T.J.; Vandekolk, T.H.; Langmead, C.J.; Danev, R.; Sexton, P.M.; Wootten, D. Cryo-EM structure of the dual incretin receptor agonist, peptide-19, in complex with the glucagon-like peptide-1 receptor. *Biochemical and Biophysical Research Communications* **2021**, *578*, 84–90, doi:10.1016/j.bbrc.2021.09.016.

32. Sun, B.; Willard, F.S.; Feng, D.; Alsina-Fernandez, J.; Chen, Q.; Vieth, M.; Ho, J.D.; Showalter, A.D.; Stutsman, C.; Ding, L.; et al. Structural determinants of dual incretin receptor agonism by tirzepatide. *Proceedings of the National Academy of Sciences* **2022**, *119*, e2116506119, doi:10.1073/pnas.2116506119.

33. Cong, Z.; Zhao, F.; Li, Y.; Luo, G.; Mai, Y.; Chen, X.; Chen, Y.; Lin, S.; Cai, X.; Zhou, Q.; et al. Molecular features of the ligand-free GLP-1R, GCGR and GIPR in complex with Gs proteins. *Cell Discov* **2024**, *10*, 1–13, doi:10.1038/s41421-024-00649-0.

34. Wang, Y.; Yang, D.; Wang, M. Signaling profiles in HEK 293T cells co-expressing GLP-1 and GIP receptors. *Acta Pharmacol Sin* **2022**, *43*, 1453–1460, doi:10.1038/s41401-021-00758-6.

35. Saxena, A.R.; Frias, J.P.; Brown, L.S.; Gorman, D.N.; Vasas, S.; Tsamandouras, N.; Birnbaum, M.J. Efficacy and Safety of Oral Small Molecule Glucagon-Like Peptide 1 Receptor Agonist Danuglipron for Glycemic Control Among Patients With Type 2 Diabetes: A Randomized Clinical Trial. *JAMA Network Open* **2023**, *6*, e2314493, doi:10.1001/jamanetworkopen.2023.14493.

36. Webb, B.; Sali, A. Comparative Protein Structure Modeling Using MODELLER. *Curr Protoc Bioinformatics* **2016**, *54*, 5.6.1-5.6.37, doi:10.1002/cpbi.3.

37. Schrödinger Release Notes - Release 2024-4 Available online: https://www.schrodinger.com/life-science/download/release-notes/ (accessed on Jan 29, 2025).

38. Jo, S.; Kim, T.; Iyer, V.G.; Im, W. CHARMM-GUI: A web-based graphical user interface for CHARMM. *Journal of Computational Chemistry* **2008**, *29*, 1859–1865, doi:10.1002/jcc.20945.

39. Lee, J.; Cheng, X.; Swails, J.M.; Yeom, M.S.; Eastman, P.K.; Lemkul, J.A.; Wei, S.; Buckner, J.; Jeong, J.C.; Qi, Y.; et al. CHARMM-GUI Input Generator for NAMD, GROMACS, AMBER, OpenMM, and CHARMM/OpenMM Simulations Using the CHARMM36 Additive Force Field. *J. Chem. Theory Comput.* **2016**, *12*, 405–413, doi:10.1021/acs.jctc.5b00935.

40. Feng, S.; Park, S.; Choi, Y.K.; Im, W. CHARMM-GUI Membrane Builder: Past, Current, and Future Developments and Applications. *J. Chem. Theory Comput.* **2023**, *19*, 2161–2185, doi:10.1021/acs.jctc.2c01246.

41. Lomize, M.A.; Pogozheva, I.D.; Joo, H.; Mosberg, H.I.; Lomize, A.L. OPM database and PPM web server: resources for positioning of proteins in membranes. *Nucleic Acids Res* **2012**, *40*, D370-376, doi:10.1093/nar/gkr703.

42. Lemkul, J.A. From Proteins to Perturbed Hamiltonians: A Suite of Tutorials for the GROMACS-2018 Molecular Simulation Package [Article v1.0]. *Living Journal of Computational Molecular Science* **2019**, *1*, 5068–5068, doi:10.33011/livecoms.1.1.5068.

43. Michaud-Agrawal, N.; Denning, E.J.; Woolf, T.B.; Beckstein, O. MDAnalysis: A toolkit for the analysis of molecular dynamics simulations. *Journal of Computational Chemistry* **2011**, *32*, 2319–2327, doi:10.1002/jcc.21787.

44. Grant, B.J.; Skjærven, L.; Yao, X.-Q. The Bio3D packages for structural bioinformatics. *Protein Science* **2021**, *30*, 20–30, doi:10.1002/pro.3923.

45. Del Conte, A.; Camagni, G.F.; Clementel, D.; Minervini, G.; Monzon, A.M.; Ferrari, C.; Piovesan, D.; Tosatto, S.C.E. RING 4.0: faster residue interaction networks with novel interaction types across over 35,000 different chemical structures. *Nucleic Acids Res* **2024**, *52*, W306–W312, doi:10.1093/nar/gkae337.

46. Wagner, J.R.; Sørensen, J.; Hensley, N.; Wong, C.; Zhu, C.; Perison, T.; Amaro, R.E. POVME 3.0: Software for Mapping Binding Pocket Flexibility. *J. Chem. Theory Comput.* **2017**, *13*, 4584–4592, doi:10.1021/acs.jctc.7b00500.

47. Liang, Y.-L.; Khoshouei, M.; Glukhova, A.; Furness, S.G.B.; Zhao, P.; Clydesdale, L.; Koole, C.; Truong, T.T.; Thal, D.M.; Lei, S.; et al. Phase-plate cryo-EM structure of a biased agonist-bound human GLP-1 receptor–Gs complex. *Nature* **2018**, *555*, 121–125, doi:10.1038/nature25773.

48. Wingler, L.M.; Elgeti, M.; Hilger, D.; Latorraca, N.R.; Lerch, M.T.; Staus, D.P.; Dror, R.O.; Kobilka, B.K.; Hubbell, W.L.; Lefkowitz, R.J. Angiotensin Analogs with Divergent Bias Stabilize Distinct Receptor Conformations. *Cell* **2019**, *176*, 468-478.e11, doi:10.1016/j.cell.2018.12.005.

49. Wootten, D.; Reynolds, C.A.; Smith, K.J.; Mobarec, J.C.; Koole, C.; Savage, E.E.; Pabreja, K.; Simms, J.; Sridhar, R.; Furness, S.G.B.; et al. The Extracellular Surface of the GLP-1 Receptor Is a Molecular Trigger for Biased Agonism. *Cell* **2016**, *165*, 1632–1643, doi:10.1016/j.cell.2016.05.023.

50. Implications of ligand-receptor binding kinetics on GLP-1R signalling. *Biochemical Pharmacology* **2022**, *199*, 114985, doi:10.1016/j.bcp.2022.114985.

51. Krumm, B.; Roth, B.L. A Structural Understanding of Class B GPCR Selectivity and Activation Revealed. *Structure* **2020**, *28*, 277–279, doi:10.1016/j.str.2020.02.004.

52. Lei, S.; Clydesdale, L.; Dai, A.; Cai, X.; Feng, Y.; Yang, D.; Liang, Y.-L.; Koole, C.; Zhao, P.; Coudrat, T.; et al. Two distinct domains of the glucagon-like peptide-1 receptor control peptide-mediated biased agonism. *J Biol Chem* **2018**, *293*, 9370–9387, doi:10.1074/jbc.RA118.003278.

53. Oqua, A.I.; Chao, K.; Eid, L.E.; Casteller, L.; Miguéns, A.; Barg, S.; Jones, B.; Serna, J.B. de la; Rouse, S.L.; Tomas, A. Molecular mapping and functional validation of GLP-1R cholesterol binding sites in pancreatic beta cells. *eLife* **2024**, *13*, doi:10.7554/eLife.101011.1.

54. Zhang, J.; Bai, Q.; Pérez-Sánchez, H.; Shang, S.; An, X.; Yao, X. Investigation of ECD conformational transition mechanism of GLP-1R by molecular dynamics simulations and Markov state model. *Phys. Chem. Chem. Phys.* **2019**, *21*, 8470–8481, doi:10.1039/C9CP00080A.

55. Ma, H.; Huang, W.; Wang, X.; Zhao, L.; Jiang, Y.; Liu, F.; Guo, W.; Sun, X.; Zhong, W.; Yuan, D.; et al. Structural insights into the activation of GLP-1R by a small molecule agonist. *Cell Res* **2020**, *30*, 1140–1142, doi:10.1038/s41422-020-0384-8.

56. Gardella, T.J.; Vilardaga, J.-P. International Union of Basic and Clinical Pharmacology. XCIII. The parathyroid hormone receptors--family B G protein-coupled receptors. *Pharmacol Rev* **2015**, *67*, 310–337, doi:10.1124/pr.114.009464.

57. Sato, T. Conserved 2nd Residue of Helix 8 of GPCR May Confer the Subclass-Characteristic and Distinct Roles through a Rapid Initial Interaction with Specific G Proteins. *IJMS* **2019**, *20*, 1752, doi:10.3390/ijms20071752.

58. Murali, S.; Aradhyam, G.K. Divergent roles of DRY and NPxxY motifs in selective activation of downstream signalling by the apelin receptor. *Biochem J* **2024**, *481*, 1707–1722, doi:10.1042/BCJ20240320.

59. Sano, F.K.; Akasaka, H.; Shihoya, W.; Nureki, O. Cryo-EM structure of the endothelin-1-ETB-Gi complex. *eLife* **2023**, *12*, e85821, doi:10.7554/eLife.85821.

60. Li, B.; Maruszko, K.; Kim, S.-K.; Yang, M.Y.; Vo, A.-D.P.; Goddard, W.A.I. Structure and Molecular Mechanism of Signaling for the Glucagon-like Peptide-1 Receptor Bound to Gs Protein and Exendin-P5 Biased Agonist. *J. Am. Chem. Soc.* **2023**, *145*, 20422–20431, doi:10.1021/jacs.3c05996.

61. El Eid, L.; Reynolds, C.A.; Tomas, A.; Ben Jones Biased agonism and polymorphic variation at the GLP-1 receptor: Implications for the development of personalised therapeutics. *Pharmacological Research* **2022**, *184*, 106411, doi:10.1016/j.phrs.2022.106411.

62. Jones, B.; Buenaventura, T.; Kanda, N.; Chabosseau, P.; Owen, B.M.; Scott, R.; Goldin, R.; Angkathunyakul, N.; Corrêa Jr, I.R.; Bosco, D.; et al. Targeting GLP-1 receptor trafficking to improve agonist efficacy. *Nat Commun* **2018**, *9*, 1602, doi:10.1038/s41467-018-03941-2.

63. Deganutti, G.; Liang, Y.-L.; Zhang, X.; Khoshouei, M.; Clydesdale, L.; Belousoff, M.J.; Venugopal, H.; Truong, T.T.; Glukhova, A.; Keller, A.N.; et al. Dynamics of GLP-1R peptide agonist engagement are correlated with kinetics of G protein activation. *Nature Communications* **2022**, *13*, 92, doi:10.1038/s41467-021-27760-0.

64. Hilger, D.; Kumar, K.K.; Hu, H.; Pedersen, M.F.; O'Brien, E.S.; Giehm, L.; Jennings, C.; Eskici, G.; Inoue, A.; Lerch, M.; et al. Structural insights into differences in G protein activation by family A and family B GPCRs. *Science* **2020**, *369*, eaba3373, doi:10.1126/science.aba3373.